AAEC/E181

AAEC/E181

AUSTRALIAN ATOMIC ENERGY COMMISSION
RESEARCH ESTABLISHMENT
LUCAS HEIGHTS

WORTH OF BORON ROD IN THE REACTOR MOATA

by

N. SPINKS

June 1967

AUSTRALIAN ATOMIC ENERGY COMMISSION

RESEARCH ESTABLISHMENT

LUCAS HEIGHTS

WORTH OF BORON ROD IN THE REACTOR MOATA

by

N. SPINKS

ABSTRACT

The U^{235} fuel increase required to compensate for the insertion in MOATA of an enriched boron rod is measured.

The DIFF code is used to calculate the mass increase and comparison with the experimental result provides a check on the theory incorporated in the code.

In addition to the experimental check, a simplified calculational mock-up of the experiment is used as the basis of a more detailed comparison between the diffusion theory and transport theory.

The worth of the rod as calculated by the diffusion theory is high by 10 per cent when compared to experiment and low by about 3 per cent when compared to transport theory.

In general, the neutron fluxes calculated by the diffusion theory agree to within 2 per cent with those from transport theory.

CONTENTS

	Page
1. INTRODUCTION	1
2. EXPERIMENTAL CRITICAL MASS	1
2.1 Shim Rod Reactivity Coefficient	1
2.2 Temperature Coefficient	1
2.3 U^{235} Mass Coefficient	2
2.4 Corrected Critical Mass	2
2.5 Reactivity Worth of B^{10} Rod	2
3. THEORETICAL ANALYSIS	2
3.1 Analytical Procedure	3
3.1.1 Spectrum calculations	3
3.1.2 Tank homogenisation	4
3.1.3 Transport calculations of the circularised geometry of the centre plane	4
3.1.4 Reduction from transport to diffusion theory	4
3.1.5 Diffusion calculation in the RZ model	4
3.2 Deficiencies in the RZ Model	5
3.3 CRAM Convergence	5
3.4 Results	6
3.5 Comparison of Diffusion Theory with Transport Theory	6
4. DISCUSSION	7
5. REFERENCES	8
6. ACKNOWLEDGMENTS	8

Table 1 Total Masses of Materials in Box

Table 2 Experimental Readings

Table 3 U^{235} Critical Mass Corrected to T = 72.5 °F, θ = 53.03 °

Table 4 Flux Discontinuity in Multiples of the Net Current

Table 5 Calculated Effective Multiplication Constant

Table 6 Comparison of Diffusion Theory with Transport Theory: Effective Multiplication Constant and Leakage

Table 7 Comparison of Diffusion Theory with Transport Theory: Volume-Integrated Flux per Uniform Region

Figure 1 Schematic Plan and Elevation of Reactor MOATA with ½ in. Diameter B^{10} Rod Inserted

Figure 2 Plan View of Fuel Distribution in MOATA Core Tanks for B^{10} Rod Experiment

Figure 3 Quadrant of Plane 'XX' (Figure 1) Comparing Actual Geometry and Cylindrical Model

(continued)

CONTENTS (continued)

Figure 4 Two-Dimensional (RZ) Model of MOATA

Figure 5 Comparison of Neutron Flux from Diffusion Theory to Neutron Flux from Transport Theory in a Radial Traverse at the Centre Plane in the RZ Model. Group 1 of 2 Neutron Energy Groups.

Figure 6 Comparison of Neutron Flux from Diffusion Theory to Neutron Flux from Transport Theory in a Radial Traverse at the Centre Plane in the RZ Model. Group 2 of 2 Neutron Energy Groups.

Figure 7 Comparison of Neutron Flux from Diffusion Theory to Neutron Flux from Transport Theory in an Axial Traverse at the Centre Line of the RZ Model. Group 1 of 2 Neutron Energy Groups.

Figure 8 Comparison of Neutron Flux from Diffusion Theory to Neutron Flux from Transport Theory in an Axial Traverse at the Centre Line of the RZ Model. Group 2 of 2 Neutron Energy Groups.

1. INTRODUCTION

The increase in U^{235} mass required to compensate for a B^{10} rod inserted centrally in the A.A.E.C.'s reactor MOATA, has been measured in collaboration with MOATA operations staff. This measurement provides a means of checking the DIFF code (Spinks and Manning 1967), the theoretical methods for which are directed at producing diffusion theory boundary conditions at control rod surfaces.

The original form of the MOATA reactor is described by Marks (1962). The reactor has since been modified to allow the insertion of a 1 foot cube aluminium box in the internal graphite reflector. In the experiment the box is loaded with eleven 1 inch BeO tiles, interleaved by ten layers of uranium foils (approximately 90% enriched) with aluminium spacers covering each interface. The B^{10} rod (10 in. long and ½ in. dia.) is located in an aluminium tube at the centre of the box. The box is inserted in MOATA with the rod axis on the E–W centre line of the reactor (Figure 1). Table 1 gives the masses of materials in the box. Figure 2 details the distribution of fuel in the two core tanks. The loadings in positions A, F, G and L are varied to obtain critical conditions for the reactor with and without the boron rod in place and Table 2 gives the loadings in these positions, together with the cooling water temperature and the shim rod critical position for each of the chronological stages of the experiment. At stage e, the shim rod sensitivity was measured as a reactivity of ± 0.059 per cent for a shim rod movement of $\pm 47.06°$.

2. EXPERIMENTAL CRITICAL MASS

After Stage a the critical mass, defined as the mass of U^{235} in the two core tanks, can be corrected for each subsequent stage using reactivity coefficients, to correspond to the water temperature and shim rod critical position of stage a which is taken as the reference stage.

Reactivity ρ depends on the mass of U^{235} in the two core tanks M, the shim rod angular position at critical θ, and the water temperature T.

Thus $$\rho = \rho(M,\theta,T),$$

and $$d\rho = \frac{\partial\rho}{\partial M}\,dM + \frac{\partial\rho}{\partial\theta}\,d\theta + \frac{\partial\rho}{\partial T}\,dT \quad . \tag{2.1}$$

The correction at critical is:

$$dM = -\frac{\frac{\partial\rho}{\partial\theta}\,d\theta + \frac{\partial\rho}{\partial T}\,dT}{\frac{\partial\rho}{\partial M}} \quad . \tag{2.2}$$

2.1 Shim Rod Reactivity Coefficient

From the shim rod calibration mentioned above,

$$\frac{\partial\rho}{\partial\theta} = \frac{0.059}{47.06} = 0.00125 \text{ \% per } °\theta \quad .$$

2.2 Temperature Coefficient

From Stages c and f of Table 2 we find the temperature coefficient. Using Equation 2.1,

$$0 = 0.00125\,(40.64 - 33.04) + \frac{\partial\rho}{\partial T}\,(75.0 - 72.6)$$

so that $$\frac{\partial\rho}{\partial T} = -0.00396 \text{ \% per } °F \quad .$$

2.3 U^{235} Mass Coefficient

From Stages b and c of Table 2 we find the mass coefficient. Using Equation 2.1 again,

$$0 = \frac{\partial \rho}{\partial M}(2510.449 - 2504.995) + 0.00125\,(33.04 - 69.3) - 0.00396\,(72.6 - 72.2)$$

so that $\frac{\partial \rho}{\partial M} = 0.00860$ % per gram.

2.4 Corrected Critical Mass

The corrected critical mass, at each stage, is presented in Table 3. An additional fuel loading of about 110 grams is required to compensate for the B^{10} rod. The variation from 109.90 grams to 111.30 grams no doubt arises in part from the change in critical mass caused by changes in the distribution of fuel. The variation will also result from experimental errors which occur for example in determining the critical shim rod position. The total variation of about ± 1% around the value 110.6 grams is sufficiently small to allow the consideration of a symmetrical fuel distribution in the theoretical analysis, and to make a more involved investigation of experimental error unnecessary.

2.5 Reactivity Worth of B^{10} Rod

The reactivity worth of the B^{10} rod can be estimated from the mass increase using the reactivity coefficient of Section 2.3. We obtain

$$\delta\rho \approx \frac{\partial \rho}{\partial M}\,\delta M$$

$$= 0.00860 \times 110.6 = 0.95\% \ .$$

The result is approximate, not only because $\frac{\partial \rho}{\partial M}$ and M are subject to experimental error, but also because $\frac{\partial \rho}{\partial M}$ is measured in the rod-in situation. $\frac{\partial \rho}{\partial M}$ might be different in the rod-out situation.

3. THEORETICAL ANALYSIS

"For many reactors it is possible to isolate, in a one-space-dimension (1D) model, that portion of the reactor configuration which requires solution at a high level of transport theory. If diffusion theory parameters are obtained so as to reproduce in diffusion theory, the essential characteristics of the 1D transport solution, then a calculation of the more realistic reactor geometry can be made at the diffusion theory level". This statement is the basis of the theory incorporated in the DIFF code. DIFF produces neutron diffusion parameters from the results of a 1D transport calculation using the WDSN code, (Francescon 1963). If the 1D calculation is repeated in diffusion theory, then in each neutron energy group the diffusion parameters preserve all reaction rates integrated over the volume of each uniform region, all boundary net currents, and the net current at each interface between uniform regions.

To analyse the experiment we choose for the 1D transport model a circularised geometry of the centre plane of the reactor. This geometry (Figure 3) is obtained by equating the circular cross sectional areas to the actual cross sectional areas in the plane X X shown in the elevation (Figure 1). The radial pitch of the four fuel rings in the 1D model is equated to the actual pitch of the enriched uranium foils.

The diffusion theory geometry (Figure 4) is an R Z model of the reactor, the Z axis corresponding to the E–W centre line. All Z dimensions are preserved in the model, the radial dimensions being chosen to preserve the volumes of the individual reactor regions.

In the RZ geometry and with the rod out, the effective multiplication constant k_0 corresponding to the measured rod-out fuel mass of 2396.195 grams is evaluated. In the rod-in situation we determine k_1 for the same mass, 2396.195 grams, and then k_2 for the measured mass increase of 110.6 grams.

The theoretical rod reactivity worth is:

$$\rho_{th} = \frac{k_0 - k_1}{k_0} . \tag{3.1}$$

The reactivity change corresponding to the measured mass increase is:

$$\rho_{exp} = \frac{k_2 - k_1}{k_2} . \tag{3.2}$$

This value is preferred to the estimated result of Section 2.5.

An exact analysis would yield:

$$k_0 = k_2 = 1$$

with the result:

$$\rho_{th} = \rho_{exp} .$$

The theoretical error is:

$$\delta\rho \equiv \rho_{th} - \rho_{exp} = \frac{k_1}{k_2 k_0} (k_0 - k_2) . \tag{3.3}$$

The fractional error is:

$$\frac{\delta\rho}{\rho_{exp}} = \frac{k_1}{k_0} \cdot \frac{k_0 - k_2}{k_2 - k_1} = (1 - \rho_{th}) \frac{k_0 - k_2}{k_2 - k_1} . \tag{3.4}$$

An alternative approach is to determine the theoretical mass increase M_{th} by linear interpolation between k_1 and k_2 to find the mass increase corresponding to k_0. This procedure yields the fractional error:

$$\frac{\delta M}{M_{exp}} = \frac{M_{th} - 110.6}{110.6} = \frac{k_0 - k_2}{k_2 - k_1} . \tag{3.5}$$

$\delta M/M_{exp}$ differs from $\delta\rho/\rho_{exp}$ by the fraction ρ_{th}, which is only 1 per cent.

3.1 Analytical Procedure

Computer codes used in the analysis are

(i) GYMEA, Pollard and Robinson (1966), for spectrum calculations,

(ii) WDSN, Francescon (1963), for transport calculations,

(iii) CRAM, Hassitt (1962), for diffusion calculations, plus, of course, DIFF.

The analysis proceeds as follows.

3.1.1 Spectrum calculations

Zero-buckling spectrum calculations are made:

(i) For the materials within the core tank.

(ii) For the materials within the box, ignoring the effect of the B^{10} rod.

The materials are considered homogeneously mixed with no allowance for spatial flux depressions except in the resonance region where effective potential scattering cross sections allow for flux depressions in the fuel lump.

The spectra are used to condense to 8 neutron energy groups the basic data for materials within the tank and for materials within the box, including the B^{10} rod. The tank spectrum is used to condense data for the water and graphite reflector regions. The groups are chosen so that they divide the box spectrum into 8 fairly equal parts.

3.1.2 Tank homogenisation

An S6 transport calculation on the tank fuel-aluminium-water slab cell is used in a flux-weighted homogenisation of the cell. In the transport calculation the buckling transverse to the cell slab co-ordinate is taken as zero. The number of directions (S6) is needed to obtain a sufficiently accurate neutron flux distribution. Homogenised diffusion coefficients are taken equal to $1/(3\bar{\Sigma}_{tr})$ where $\bar{\Sigma}_{tr}$ is the flux-weighted transport cross section. Such a prescription is valid for the thin tank cell (Benoist 1959).

3.1.3 Transport calculations of the circularised geometry of centre plane

Two S6 transport calculations, one for the rod-in and one for the rod-out situation, are made for the circularised geometry of the centre plane (Figure 3). Zero inflow of neutrons is taken as the boundary condition at the outer radius of the graphite. Zero buckling in the transverse direction is assumed.

3.1.4 Reduction from transport to diffusion theory

DIFF is used to produce two sets of diffusion theory parameters from the results of the two transport calculations of Section 3.1.3.

In the rod-out case, DIFF is used to smear all materials up to the graphite interface. Diffusion coefficients in the smeared region are taken to equal $1/(3\bar{\Sigma}_{tr})$ where $\bar{\Sigma}_{tr}$ is the flux-weighted average transport cross section. Diffusion coefficients in the graphite region are determined by the DIFF method of fitting a diffusion flux to the transport flux. In addition to the two sets of 8-group macroscopic cross sections for the graphite and smeared regions, DIFF produces boundary conditions in each group at the outer radius of the graphite, and flux discontinuity conditions in each group at the graphite interface.

In the rod-in case, DIFF is used to smear all materials from the rod surface to the graphite interface. In addition to the quantities produced in the rod-out case DIFF gives the boundary condition, in each group, at the rod surface.

3.1.5 Diffusion calculation in the RZ model

Diffusion theory calculations of the more realistic RZ model are made for:

(i) the unmodified MOATA (graphite instead of box),

(ii) MOATA with box but rod-out, and

(iii) MOATA with box but rod-in.

As mentioned before, the mass of U^{235} in the core tank is varied from calculation to calculation. Two separate loadings are considered in the rod-in case. The mass variation is achieved by varying the dimension t of Figure 4. Examining the real situation (Figure 2), we see that some correspondence is achieved between the experimental and calculational addition of fuel.

Calculations are made on the unmodified MOATA system to examine those deficiencies in the model which are independent of the box representation.

3.2 Deficiencies in the RZ Model

A problem with the RZ model is the treatment of the outer reflector regions at values of the Z co-ordinate corresponding to the fuel tanks. Referring to Figure 1, in plan view this region is graphite, but in elevation it is water, the cooling water in the inlet and outlet channels. We choose, in the model, a homogeneous mixture of graphite and water so as to preserve the actual quantities. Since the flux attenuates more rapidly in water than in graphite, less weight should be given to the water. Giving too much weight to the poorer reflector will result in the model tending to underestimate reactivity.

Another problem is to allow for the presence in each core tank of some 5000 grams of stainless steel in the form of a lifting lug and two pins for each of the six fuel assemblies. The difficulty lies in determining shielding factors for the steel lumps. If shielding is ignored and the steel is uniformly smeared through the core tank then reactivity will be underestimated. If the steel itself is ignored reactivity will be overestimated.

Though the shim rod reference position is 53.03°, the shim rod is not inserted, that is, $\theta = 300°$ for the calculation. From MOATA calibration curves (Marks 1966), this effect should cause the model to overestimate reactivity by 0.52 per cent.

In the calculations the reactor temperature was taken as 162.5 °F instead of the reference temperature of 72.5 °F. The temperature coefficient of Section 2.2 indicates a resulting underestimation of reactivity by 0.36 per cent.

The net effect of the error in temperature and the omission of the shim rod is a slight reactivity overestimation of 0.16 per cent by the model. If the steel is ignored in the model the reactivity effect will tend to cancel the effect of the treatment of the water region. The net effect on reactivity of the four error sources, that is the shim rod, the temperature, the steel and the water, is isolated from the effect of any errors in the treatment of box and rod (Sections 3.1.3 and 3.1.4), by the RZ diffusion calculation of the unmodified reactor as described by Marks (1962).

Using reactivity coefficients supplied by Marks (1966) the critical mass of 3016 grams (Marks 1962) is corrected to the reference shim rod position and the reference temperature of the experiment. The resulting 3094 gram critical mass produces an effective multiplication constant $k = 1.000$ to 1.001. (The range of values shows the degree of convergence of the diffusion calculation). With the unshielded steel included we obtain $k = 0.959$ to 0.960.

It seems likely that the steel is highly shielded and that the reactivity error from the treatment of the water region is small. Though there is still the possibility that significant compensating effects are present, we ignore the steel in the analysis of the experiment.

3.3 CRAM Convergence

Though convergence was obtained for the RZ rod-in calculation, CRAM would not converge when flux discontinuity conditions were applied at the graphite interface in the RZ rod-out case. Convergence of the RZ rod-out calculation was obtained when the discontinuity was removed. With the flux discontinuity conditions removed, preservation of the detailed reaction rates and leakages cannot be guaranteed if the 1D calculation is repeated in diffusion theory. In particular the 1D diffusion solution will not reproduce the transport value of k. Accordingly an error will be introduced in the RZ rod-out calculation.

Table 4 compares the flux discontinuity for the rod-in case with the discontinuity for the rod-out case. The discontinuity is presented in multiples of the net current at the interface. The discontinuities are quite similar, except for groups 7 and 8 where the effect of rod absorption produces significant differences. Hence the effect on k of the discontinuity in the rod-out case can be expected to be similar to the effect on k of the discontinuity in the rod-in case. This has been verified by diffusion calculations with the discontinuity removed. For the 1D rod-in case,

removal of the flux discontinuity reduced k by 0.95 per cent. For the 1D rod-out case, k was reduced by 1.12 per cent. For the RZ rod-in case, removal of the discontinuity reduced k by 0.11 per cent. Consequently, for the rod-out case, removal of the flux discontinuity should reduce k by about 0.13 per cent.

3.4 Results

Computed effective multiplication constants are presented in Table 5. The result k_0, for the rod-out case, is corrected by adding 0.0013, see Section 3.3.

From Equations 3.1 to 3.5 we obtain:

$$\rho_{th} = \begin{pmatrix} 1.13 \\ 1.11 \end{pmatrix} \% \quad ,$$

$$\rho_{exp} = \begin{pmatrix} 1.04 \\ 1.01 \end{pmatrix} \% \quad ,$$

$$\frac{\delta\rho}{\rho_{exp}} = \frac{\delta M}{M_{exp}} = \begin{pmatrix} 0.11 \\ 0.08 \end{pmatrix} \quad .$$

3.5 Comparison of Diffusion Theory with Transport Theory

An additional and more detailed check on the DIFF diffusion theory can be made by comparing the results of diffusion theory to the results of a transport theory calculation. We choose the RZ model of the MOATA experiment for this check but simplify the problem so as to make feasible the use of the TDC transport theory code (Rodgers and Check 1965). The simplifications are:

(i) The energy variable is condensed, using the spectrum calculations of Section 3.1.1, to 2 neutron energy groups.

(ii) Spatial flux depressions in the core tank uranium and in the box uranium are ignored, allowing the core tank and box to be homogenised directly from the spectrum calculations.

The simplified problem is solved in both diffusion and transport theory. The geometry and macroscopic cross sections are identical for the two calculations, though the diffusion calculation requires in addition the diffusion coefficients and the boundary and interface conditions. These additional parameters are supplied by DIFF from the results of a 2-group 1D transport calculation of the geometry at the centre plane of the simplified RZ model.

The comparison between diffusion and transport theory is made for the rod-in case only. The mass of U^{235} in the core tanks is 2506.8 grams, the measured mass in the rod-in situation.

Table 6 compares the effective multiplication constant, the leakages from the external boundary of the reactor, and the leakages into the boron rod. Table 7 compares the scalar fluxes integrated over the volume of the various uniform regions (see Figure 4). Figures 5 and 6 compare the flux distributions in a radial traverse at the centre plane. Figures 7 and 8 compare the flux distributions in an axial traverse along the centre line. The quantities are normalised throughout so that the total loss of neutrons, by absorption and leakage is 1 per second. Alternatively the results can be interpreted as being normalised to a total production of neutrons from fission equal to k per second, where k is the diffusion or transport effective multiplication constant.

The flux differences are generally too small to show up when diffusion and transport fluxes are plotted together. Instead the percentage error in the diffusion flux is plotted along with the diffusion flux in Figures 5 to 8. No attempt is made to draw a smooth curve through the discrete values of the error at each mesh point because, in fine scale, there is an apparent correlation between the mesh and the error. In particular the axial traverses, Figures 7 and 8, show the error oscillating in phase with the mesh. The axial mesh seems to be too coarse around the inner reflector region.

In Figures 5 and 6, the percentage error of the diffusion flux in the 1D model is plotted along with the percentage error at the centre plane in the RZ model. The percentage error in the 1D model is calculated from the results of a diffusion calculation in the 1D model and from the results of the transport calculation in the 1D model.

4. DISCUSSION

The increased mass of U^{235} in the MOATA core tank required to compensate for the insertion of a central B^{10} rod is measured as 110.6 grams to an accuracy of about ± 1 per cent. Calculations using the DIFF code give agreement to within about 10 per cent, the calculated mass increase being greater than the measured mass increase.

The calculated reactivity change corresponding to the measured mass increase is about 1.02 per cent. This compares favourably with the result of 0.95 per cent. obtained from the experimentally determined reactivity coefficient, and supports the accuracy of corrections made to the measured critical mass using the experimentally determined reactivity coefficients.

Comparing the results of a 2-group diffusion theory calculation on a simplified RZ model of the rod-in experimental situation with the results of a 2-group transport theory calculation on the same RZ model we find general agreement between leakages and fluxes to 1 or 2 per cent. More specifically,

(i) The diffusion theory effective multiplication constant is low by about 1 per cent.

(ii) The total neutron leakage from external boundaries agrees very accurately though the individual group-dependent leakages vary by about 2 per cent.

(iii) The group-dependent leakages into the boron rod are low, in diffusion theory, by as much as 8 per cent though the total leakage into the rod is low by only 3 per cent.

(iv) The volume-integrated fluxes in the various uniform regions are, except for the small non-fissile region within the core tank, in agreement to within 2 per cent. The volume-integrated fluxes in diffusion theory are low in fissile regions and high in non-fissile regions. Thus most of the error can be visualized as being in the low diffusion theory multiplication constant.

(v) Flux plots in the centre plane and on the centre line agree in general to within 2 per cent, though as expected, much larger discrepancies exist in the transient regions near the boron rod and the external boundary.

(vi) A discrepancy exists in a comparison between the radial plot of the percentage error in the group 2 diffusion flux from the RZ model and the corresponding plot for the 1D model. (Figure 6). The transient in the group 2 flux near the boron rod is much greater in the 1D calculation than in the RZ calculation though the transients of the group 1 flux agree well (Figure 5). This discrepancy is similar to the error in the leakage into the boron rod. The group 2 leakage error is significantly greater than the group 1 error (Table 6).

In general the comparison between diffusion and transport theory is good, though some doubt remains about the effect on the comparison of the fairly coarse finite difference mesh needed for the transport calculation and used for both the transport and diffusion calculations. It is likely that a significant portion of the difference between transport and diffusion theory is caused by the coarse mesh. The discrepancy between the group 2 flux transients can be explained only on the basis of differences between the transport codes used for the 1D and RZ calculations. Such differences will arise when the mesh is too coarse. For nearly every quantity under comparison, it is unlikely that the error due to the coarse mesh has cancelled the error inherent in the diffusion theory.

The most important single quantity compared between diffusion and transport theory is the neutron leakage into the boron rod. It is not surprising that the proportion of neutrons absorbed by the rod (0.8 per cent) is near the reactivity worth of the rod (1.0 per cent). The error in the neutron leakage into the rod is a measure of the accuracy of the diffusion theory in calculating rod reactivity worth. The error of −3 per cent is in the opposite direction to the difference between diffusion theory rod worth and the experimental rod worth of +10 per cent (Section 3.4). Thus the diffusion theory result lies between experiment and transport theory.

The analysis is a stringent test of the DIFF theory. DIFF relies on the isolation of transport effects in a 1D model of the reactor and can be confidently applied if the 1D model is a good representation of the reactor. In the analysis of the experiment, the chosen 1D model is not a good representation of the reactor since it ignores completely the effect of the MOATA core tanks on the flux distribution near the B^{10} rod. Yet the diffusion theory boundary conditions at the rod surface, obtained by DIFF from the 1D model, yield an accurate worth for the rod. Apparently the boundary conditions are little affected by deficiencies in the 1D model.

For most power reactors better 1D models exist for the isolation of transport effects in and around control rods. For control rod arrays the super-cell is quite satisfactory and the methods of DIFF could be applied with confidence.

Convergence difficulties resulting from the use of the DIFF – CRAM combination occur in applying the combination for analysis of the experiment. Fortunately CRAM converges for the rod-in calculation and it is possible to correct the multiplication constant for the rod-out calculation.

5. REFERENCES

Benoist, P. (1959). – The general formulation and practical calculation of the diffusion coefficient in a lattice containing cavities. CEA–1354 (translated by Liz Appleby in HW–TR–25).

Francescon, S. (1963). – The Winfrith DSN programme. AEEW–R273.

Hassitt, A. (1962). – A computer program to solve the multigroup diffusion equations. TRG Report 229 (R).

Marks, A. (1962). – MOATA reactor. Atomic Energy in Australia, 5(4) pp 9–21.

Marks, A. (1966). – Private communication.

Pollard, J.P., and Robinson, G.S. (1966). – GYMEA, a nuclide depletion, space independent, multigroup neutron diffusion, data preparation code. AAEC/E147.

Rodgers, R.J., and Check, P.S. (1965). – Users guide to FORTRAN TDC. TIM No. 890. Pratt and Whitney Aircraft – Canel.

Spinks, N., and Manning, G. (1967). – DIFF, a code to prepare diffusion theory parameters from the results of WDSN. AAEC/E174.

6. ACKNOWLEDGMENTS

The author gives thanks to the MOATA operations team for assistance during the experiment.

TABLE 1

TOTAL MASSES OF MATERIALS IN BOX

BeO	Al	U^{235}	B^{10}
73826 g	4927 g	804.30 g	18.5 g

TABLE 2

EXPERIMENTAL READINGS

Stage	Mass of U^{235} (gram)					Temperature of Cooling Water (°F)	Critical Position of Shim Rod (°θ)	Comment
	Core Tank Position				Total in Core Tanks			
	A	F	G	L				
a	65.800	87.430	65.800	65.560	2396.195	72.5	53.03	Rod out
b	109.480	87.430	108.930	87.080	2504.995	72.2	69.30	Rod in
c	109.480	87.430	108.930	92.534	2510.449	72.6	33.04	Rod in
d	87.430	109.480	108.930	92.534	2510.449	72.95	29.07	Rod in
e	109.480	92.539	108.930	87.430	2510.449	73.25	25.55	Rod in
f	109.480	87.430	108.930	92.534	2510.449	75.0	40.64	Rod in

TABLE 3

U^{235} CRITICAL MASS CORRECTED TO T = 72.5 °F, θ = 53.03 °

Stage	Mass (gram)	Increase (gram)
b	2507.50	111.30*
c	2507.50	111.30*
d	2506.77	110.57
e	2506.10	109.90
f	2507.50	111.30*

*Values agree since these stages are the basis for the critical mass corrections.

TABLE 4

FLUX DISCONTINUITY* IN MULTIPLES OF THE NET CURRENT

Group		1	2	3	4	5	6	7	8
$\frac{\delta\phi}{J}$ †	rod in	0.85	−0.02	−0.83	−1.02	−0.87	−0.51	−2.03	−0.46
	rod out	0.75	−0.16	−0.98	−1.14	−0.94	−0.50	−5.42	−1.06

* as determined by DIFF for the cylindrical interface between box and graphite in the RZ model

† positive when the discontinuity produces a decrease in flux in the direction of positive net current

TABLE 5

CALCULATED EFFECTIVE MULTIPLICATION CONSTANT

Reactor	Mass of U^{235} in Core Tanks (gram)	k
MOATA with Box, Rod Out	2396.20	(1.0025)* (1.0024) k_0
MOATA with Box, Rod In	2396.20	(0.9913) (0.9912) k_1
MOATA with Box, Rod In	2506.80	(1.0016) (1.0014) k_2

*The amount $\delta k_0 = 0.0013$ see Section 3.3, has been added to the CRAM results to account for the omission of flux discontinuity conditions from the rod-out calculation.

TABLE 6

COMPARISON OF DIFFUSION THEORY WITH TRANSPORT THEORY:

EFFECTIVE MULTIPLICATION CONSTANT AND LEAKAGE

Quantity to be Compared	Diffusion	Transport	Error (%)
Effective Multiplication Constant	1.049	1.058	−0.88
Leakage from External Boundary, Group 1	0.0651	0.0667	−2.39
" " " " , Group 2	0.1211	0.1193	+1.50
" " " " , Total	0.1862	0.1860	+0.11
Leakage into Boron Rod, Group 1	0.00577	0.00584	−1.20
" " " " , Group 2	0.00211	0.00229	−7.86
" " " " , Total	0.00788	0.00813	−3.08

TABLE 7

COMPARISON OF DIFFUSION THEORY WITH TRANSPORT THEORY:

VOLUME-INTEGRATED FLUX PER UNIFORM REGION

Region	Volume Integrated Flux (n cm s^{-1})					
	Group 1			Group 2		
	Diffusion	Transport	Error (%)	Diffusion	Transport	Error (%)
Box (U + BeO + Al)	8.95	8.99	−0.40	3.82	3.86	−0.95
Inner and Outer Reflector (C)	41.04	40.66	+0.94	64.33	63.65	+1.07
Tank (U + H_2O + Al)	15.01	15.16	−0.97	10.39	10.48	−0.88
Tank (H_2O + Al)	1.65	1.58	+4.55	2.35	2.24	+4.81
Side Reflector (C + H_2O + Al)	5.32	5.21	+2.01	14.46	14.23	+1.66

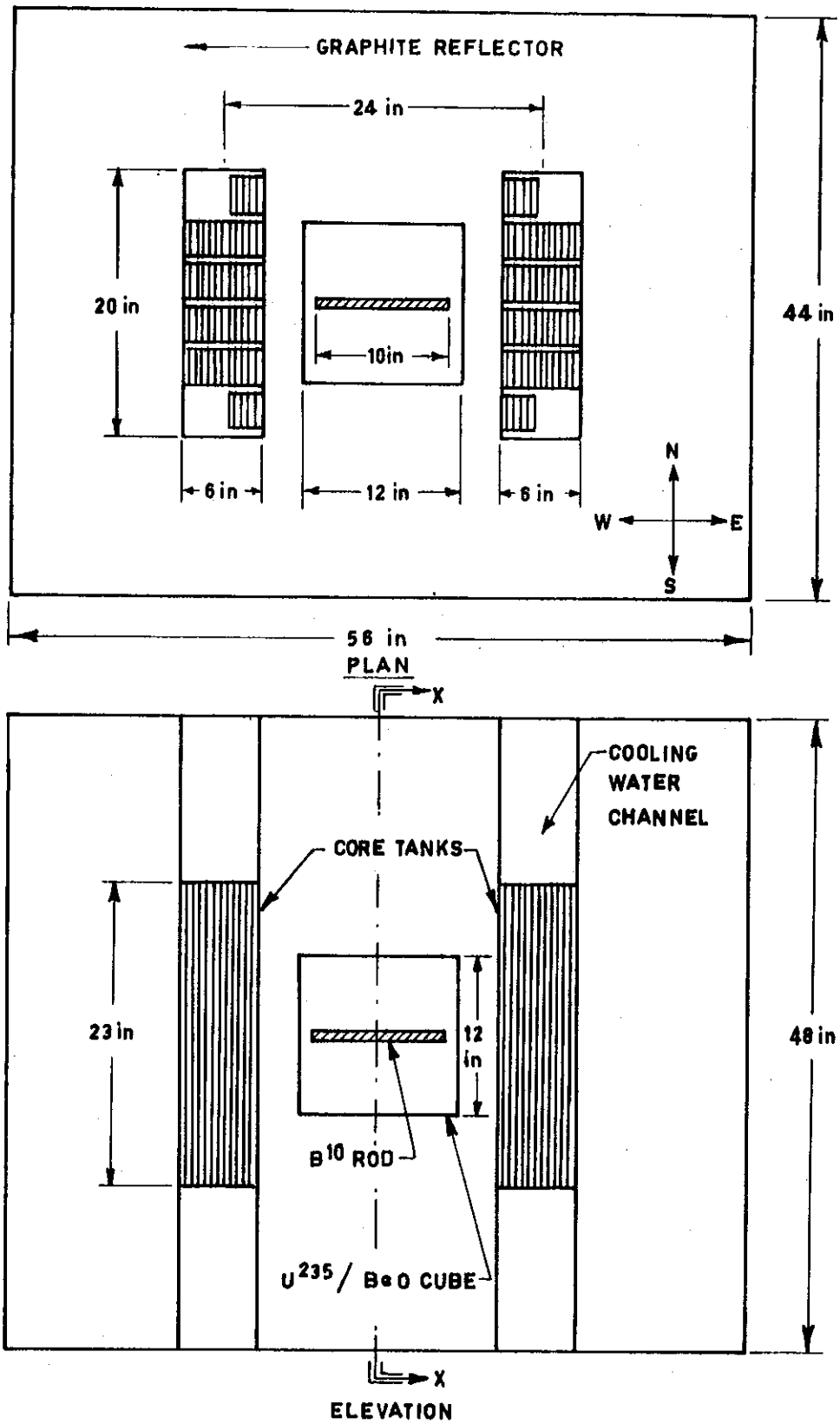

FIGURE 1. SCHEMATIC PLAN AND ELEVATION OF REACTOR 'MOATA' WITH ½ INCH DIAMETER B^{10} ROD INSERTED

P1074

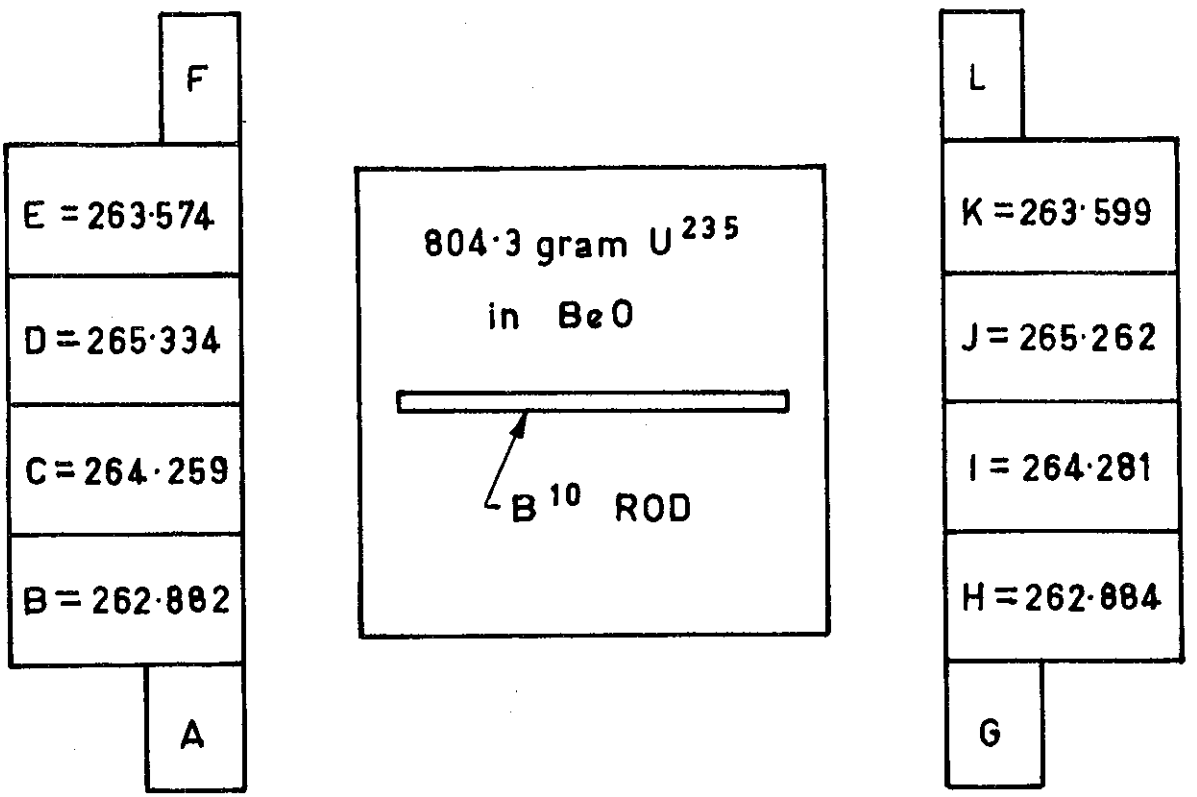

A to L are Fuel Boxes. Quantities are in grams of U^{235}

FIGURE 2. PLAN VIEW OF FUEL DISTRIBUTION IN 'MOATA' CORE TANKS FOR B^{10} ROD EXPERIMENT

P1074

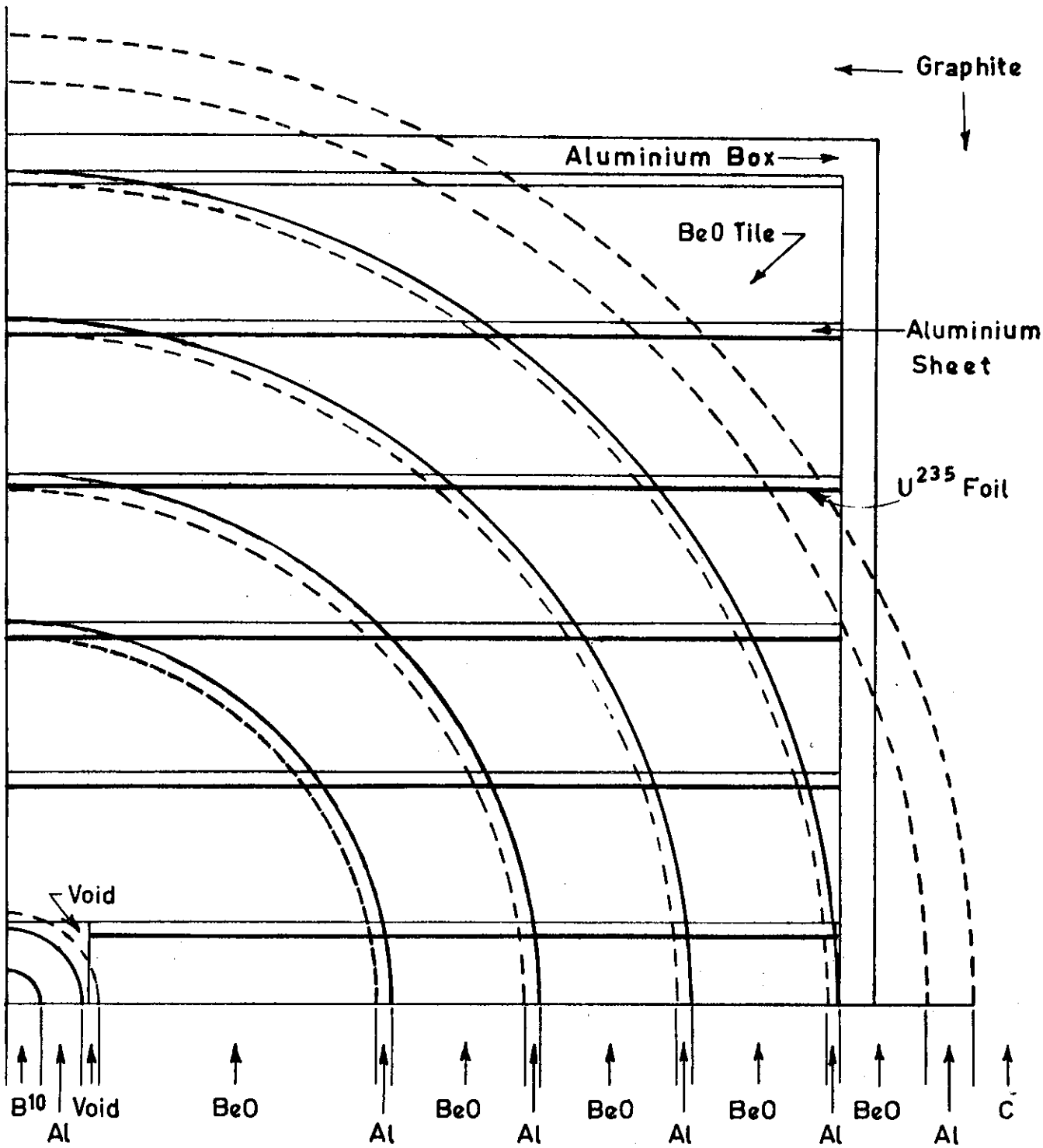

FIGURE 3. QUADRANT OF PLANE 'XX' (Figure 1) COMPARING ACTUAL GEOMETRY AND CYLINDRICAL MODEL

P1074

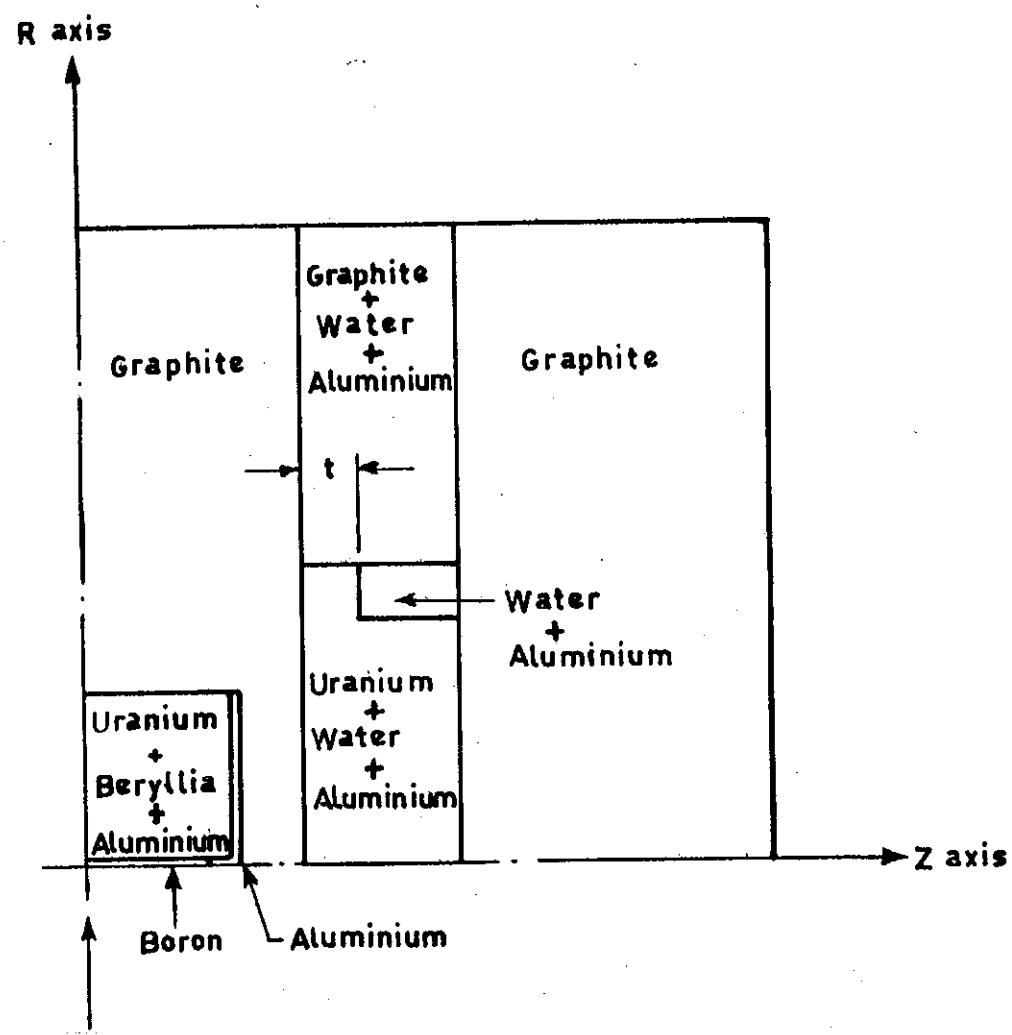

Model taken as symmetric about centre plane. Fuel mass varied by varying dimension t

FIGURE 4. TWO-DIMENSIONAL (RZ) MODEL OF MOATA

P1074

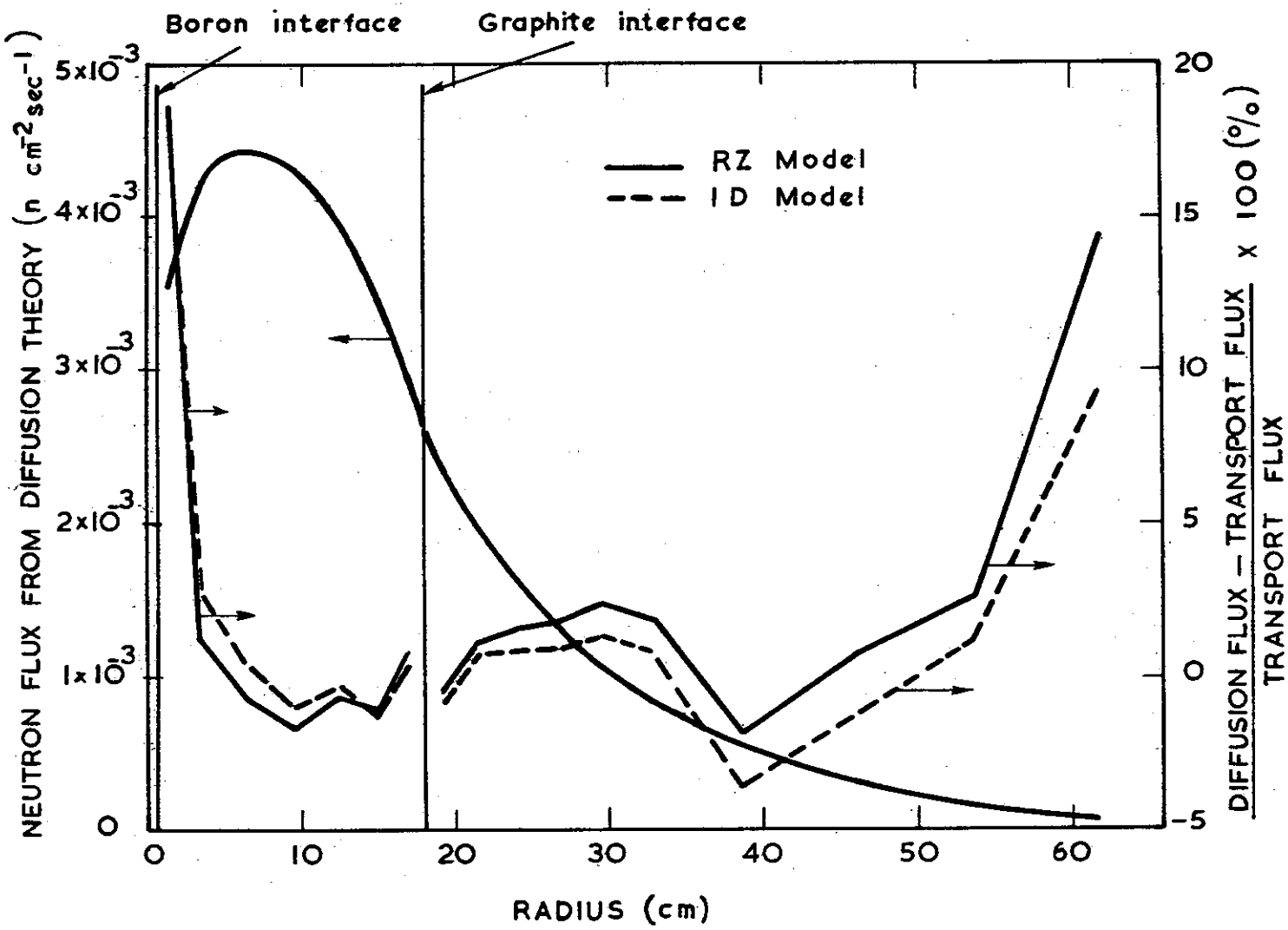

FIGURE 5. COMPARISON OF NEUTRON FLUX FROM DIFFUSION THEORY TO NEUTRON FLUX FROM TRANSPORT THEORY IN A RADIAL TRAVERSE AT THE CENTRE PLANE IN THE RZ MODEL. GROUP 1 OF 2 NEUTRON ENERGY GROUPS

P1096

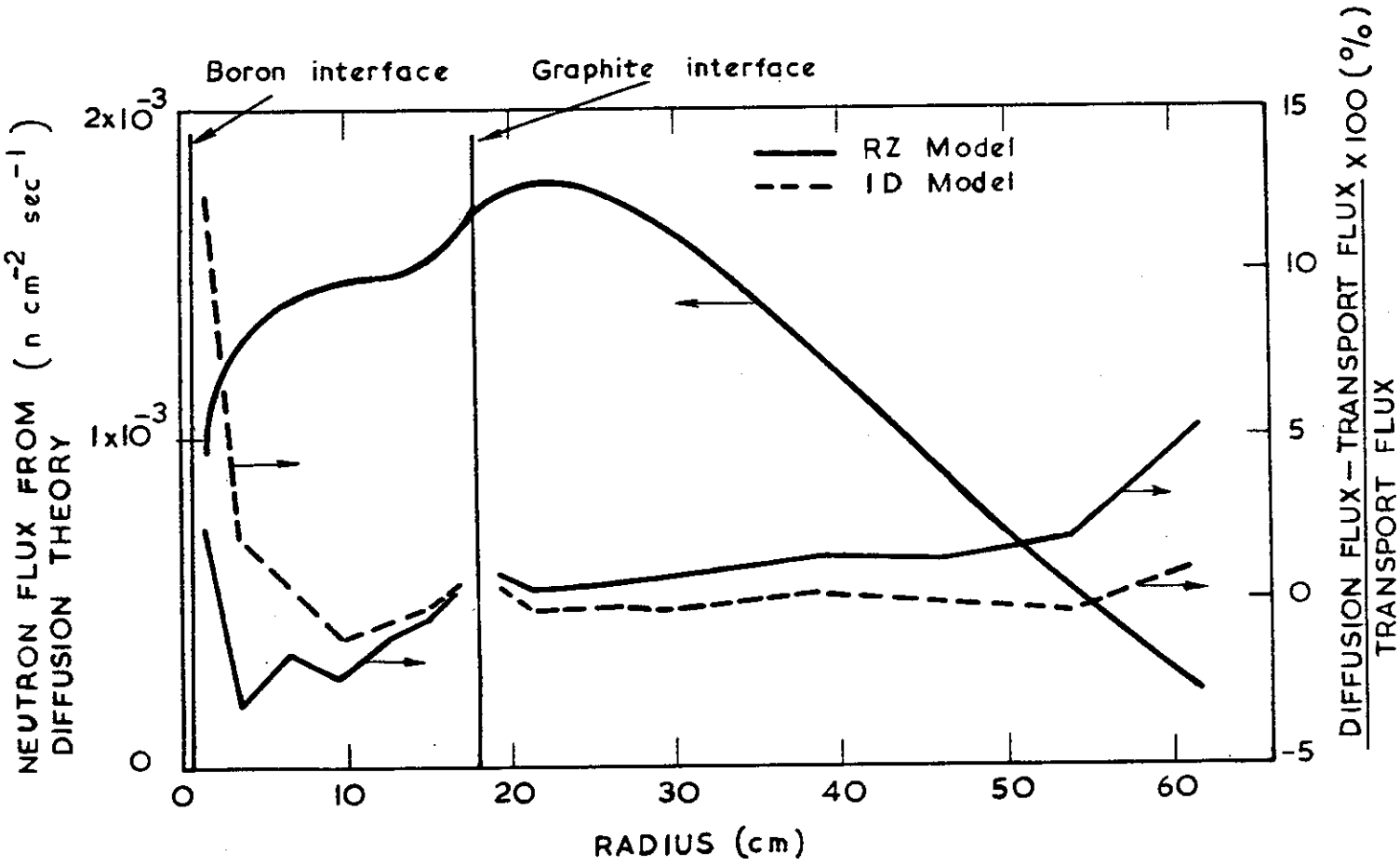

FIGURE 6. COMPARISON OF NEUTRON FLUX FROM DIFFUSION THEORY TO NEUTRON FLUX FROM TRANSPORT THEORY IN A RADIAL TRAVERSE AT THE CENTRE PLANE IN THE RZ MODEL. GROUP 2 OF 2 NEUTRON ENERGY GROUPS

P1096

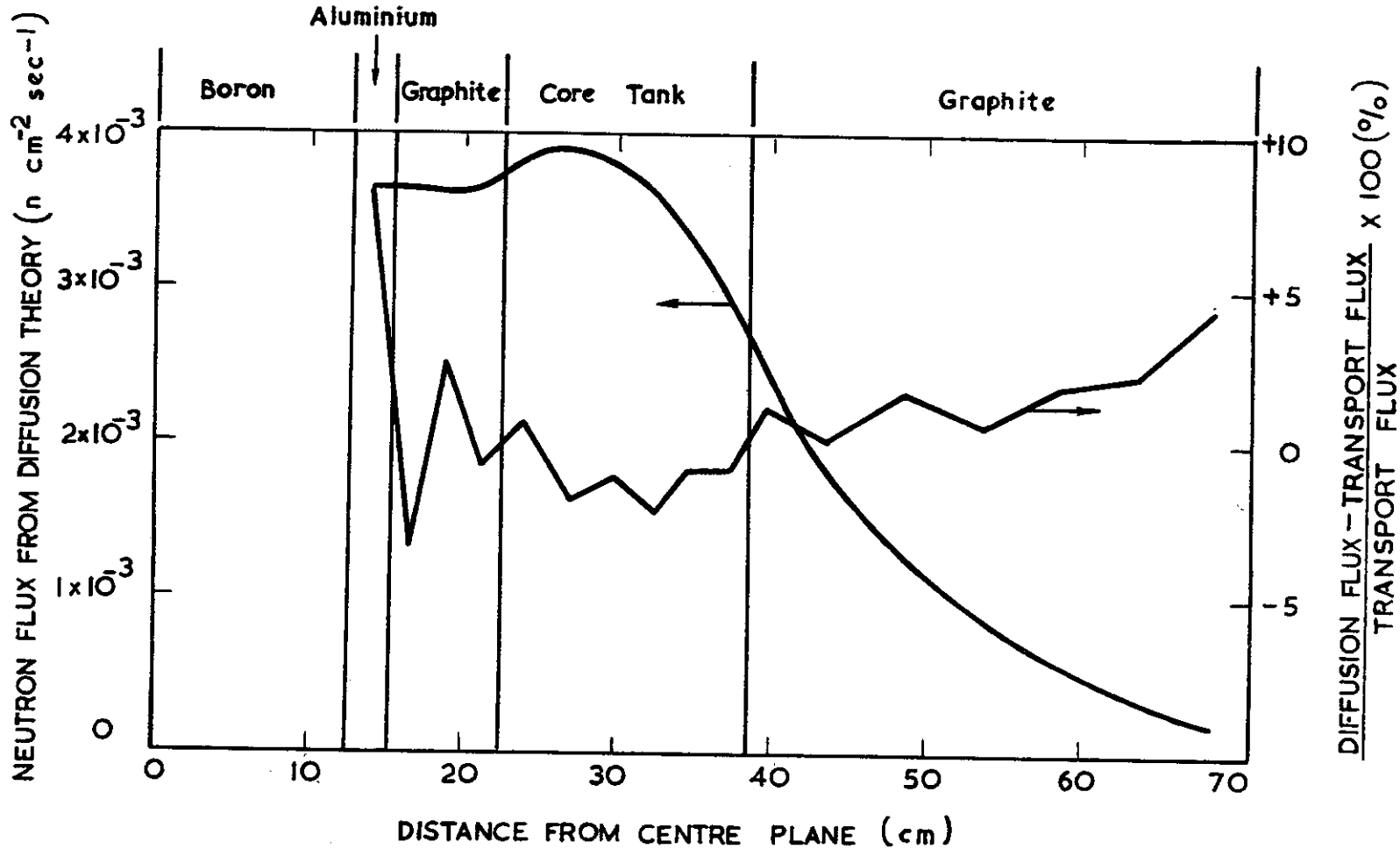

FIGURE 7. COMPARISON OF NEUTRON FLUX FROM DIFFUSION THEORY TO NEUTRON FLUX FROM TRANSPORT THEORY IN AN AXIAL TRAVERSE AT THE CENTRE LINE OF THE RZ MODEL. GROUP 1 OF 2 NEUTRON ENERGY GROUPS

P1096

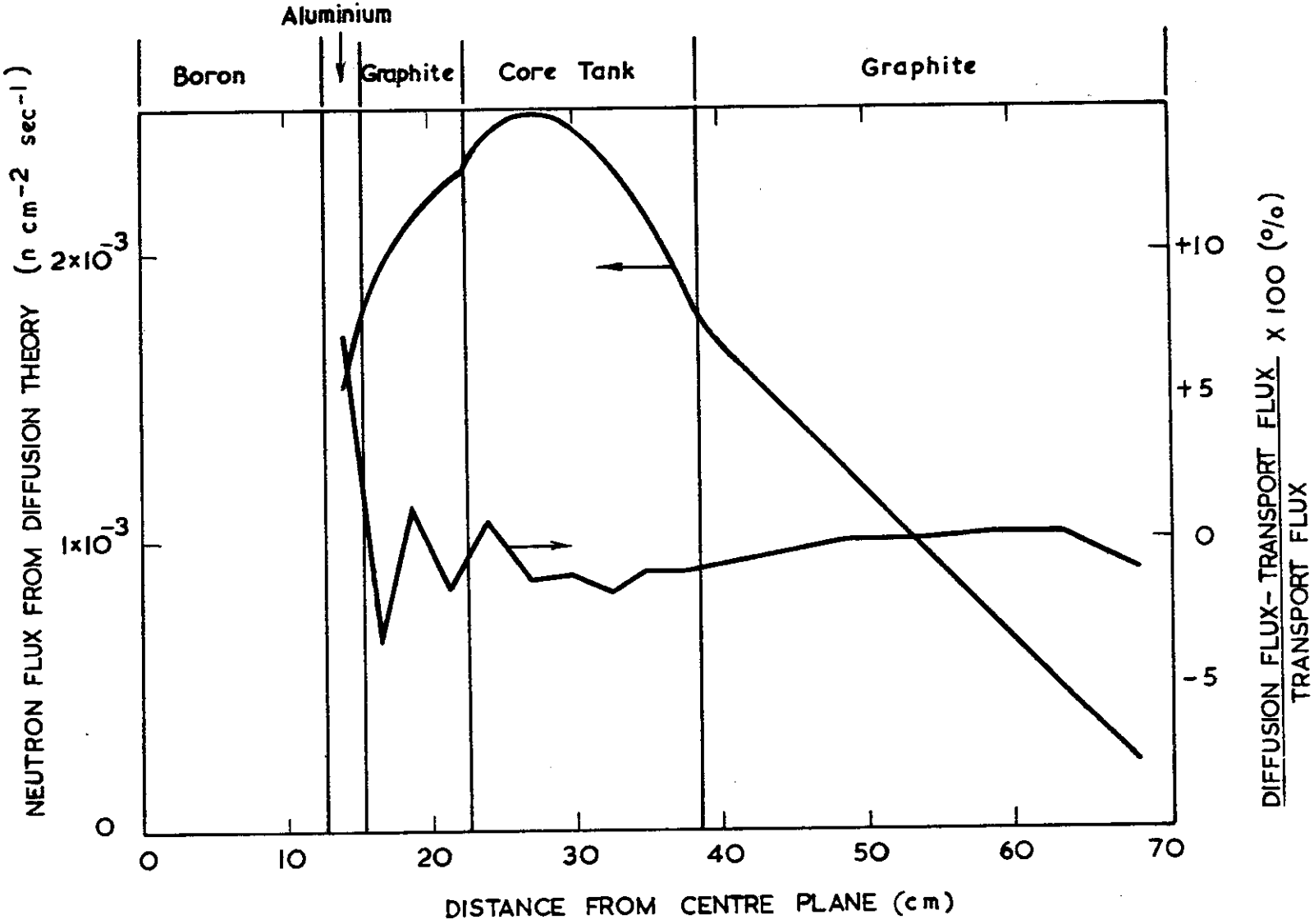

FIGURE 8. COMPARISON OF NEUTRON FLUX FROM DIFFUSION THEORY TO NEUTRON FLUX FROM TRANSPORT THEORY IN AN AXIAL TRAVERSE AT THE CENTRE LINE OF THE RZ MODEL. GROUP 2 OF 2 NEUTRON ENERGY GROUPS

P1096